

24 Abstract

25 The sea anemone, *Exaiptasia diaphana*, commonly known as *Exaiptasia pallida* or *Aiptasia*
26 *pallida*, has become increasingly popular as a model for cnidarian-microbiome symbiosis
27 studies due to its relatively rapid growth, ability to reproduce sexually and asexually, and
28 symbiosis with diverse prokaryotes and the same microalgal symbionts (family
29 Symbiodiniaceae) as its coral relatives. Clonal *E. diaphana* strains from Hawaii, the Atlantic
30 Ocean, and Red Sea are now established for use in research. Here, we introduce Great Barrier
31 Reef (GBR)-sourced *E. diaphana* strains as additions to the model repertoire. Sequencing of
32 the 18S rRNA gene confirmed the anemones to be *E. diaphana* while genome-wide single
33 nucleotide polymorphism analysis revealed four distinct genotypes. Based on *Exaiptasia*-
34 specific inter-simple sequence repeat (ISSR)-derived sequence characterized amplified region
35 (SCAR) marker and gene loci data, these four *E. diaphana* genotypes are distributed across
36 several divergent phylogenetic clades with no clear phylogeographical pattern. The GBR *E.*
37 *diaphana* genotypes comprised three females and one male, which all host *Breviolum*
38 *minutum* as their homologous Symbiodiniaceae endosymbiont. When acclimating to an
39 increase in light levels from 12 to 28 $\mu\text{mol photons m}^{-2} \text{s}^{-1}$, the genotypes exhibited
40 significant variation in maximum quantum yield of Symbiodiniaceae photosystem II and
41 Symbiodiniaceae cell density. The comparatively high levels of physiological and genetic
42 variability among GBR anemone genotypes makes these animals representative of global *E.*
43 *diaphana* diversity and thus excellent model organisms. The addition of these GBR strains to
44 the worldwide *E. diaphana* collection will contribute to cnidarian symbiosis research,
45 particularly in relation to the climate resilience of coral reefs.

46 1 Introduction

47 1.1 Coral Reefs

48 The Great Barrier Reef (GBR) contains abundant and diverse biota, including more than 300
49 species of stony corals (Fabricius et al. 2005), making it one of the most unique and complex
50 ecosystems in the world. In addition to its tremendous environmental importance, the GBR's
51 social and economic value is estimated at \$A56 billion, supporting 64,000 jobs and injecting
52 \$A6.4 billion into the Australian economy annually (O'Mahony et al. 2017).

53 Coral reef waters are typically oligotrophic, but stony corals thrive in this environment and
54 secrete the calcium carbonate skeletons that create the physical structure of the reef. Corals
55 achieve this through their symbiosis with single-celled algae of the family Symbiodiniaceae
56 that reside within the animal cells and provide the host with most of its energy (Muscatine
57 and Porter 1977). Additional support is provided by communities of prokaryotes, and
58 possibly by other microbes such as viruses, fungi and endolithic algae living in close
59 association with coral. This entity, comprising the host and its microbial partners, is termed
60 the holobiont (Rohwer et al. 2002). During periods of extreme thermal stress, the coral-
61 Symbiodiniaceae relationship breaks down. Stress-induced cellular damage creates a state of
62 physiological dysfunction, which leads to separation of the partners and, potentially, death of
63 the coral animal. This process, 'coral bleaching', is a substantial contributor to coral cover
64 loss globally (Baird et al. 2009; De'ath et al. 2012; Eakin et al. 2016; Hughes et al. 2017;
65 Hughes et al. 2018).

66 1.2 *Exaiptasia diaphana*

67 Model systems are widely used to explore research questions where experimentation on the
68 system of interest has limited feasibility or ethical constraints. Established model systems,
69 such as *Drosophila melanogaster* and *Caenorhabditis elegans*, have played crucial roles in
70 the progress of understanding organismal function and evolution in the past 50 years (Davis
71 2004). The coral model *Exaiptasia diaphana* was formally proposed by Weis et al. (2008) as
72 a useful system to study cnidarian endosymbiosis and has since achieved widespread and
73 successful use.

74 *E. diaphana* is a small sea anemone (≤ 60 mm long) found globally within temperate and
75 tropical marine shallow-water environments (Grajales and Rodriguez 2014). Originally
76 positioned taxonomically within the genus *Aiptasia*, *E. diaphana* and twelve other *Aiptasia*

77 species were combined into a new genus, *Exaiptasia* (Grajales and Rodriguez 2014).
78 Although *Exaiptasia pallida* was proposed as the taxonomic name for the twelve
79 synonymized species, the International Commission on Zoological Nomenclature (ICZN)
80 ruled against this because the species epithet *diaphana* (Rapp 1829) predated *pallida* (Verrill
81 1864) and therefore had precedence according to the Principle of Priority (ICZN 2017).

82 *E. diaphana* was first used to study cellular regeneration (Blanquet and Lenhoff 1966), with
83 its systematic use in the study of cnidarian-algal symbioses dating back to 1976 when the
84 regulation of *in hospite* Symbiodiniaceae density was explored (Steele 1976). Since then,
85 studies using *E. diaphana* have focused on the onset, maintenance, and disruption of
86 symbiosis with Symbiodiniaceae (Belda-Baillie et al. 2002; Fransolet et al. 2014; Bucher et
87 al. 2016; Hillyer et al. 2017; Cziesielski et al. 2018). *E. diaphana* has also been used in
88 studies of toxicity (Duckworth et al. 2017; Howe et al. 2017), ocean acidification (Hoadley et
89 al. 2015), disease and probiotics (Alagely et al. 2011), and cnidarian development (Chen et
90 al. 2008; Grawunder et al. 2015; Carlisle et al. 2017). Key differences between corals and *E.*
91 *diaphana* are the absence of a calcium carbonate skeleton, the constant production of asexual
92 propagates, and the greater ability to survive bleaching events in the latter. These features
93 allow researchers to use *E. diaphana* to investigate cellular processes that would otherwise be
94 difficult with corals, such as those that require survival post-bleaching to track re-
95 establishment of eukaryotic and prokaryotic symbionts. Further, adult anemones can be fully
96 bleached without eliciting mortality, which is often difficult for corals, thus providing a
97 system for algal reinfection studies independent of sexual reproduction and aposymbiotic
98 larvae.

99 Three strains of *E. diaphana* currently dominate the research field as models for coral
100 research. H2 (female) was originally collected from Coconut Island, Hawaii, USA (Xiang et
101 al. 2013), CC7 (male) from the South Atlantic Ocean off North Carolina, USA (Sunagawa et
102 al. 2009) and RS (female, pers.comm., but see (Schlesinger et al. 2010)) collected from the
103 Red Sea at Al Lith, Saudi Arabia (Cziesielski et al. 2018). The majority of *E. diaphana*
104 resources have been developed from the clonal line, CC7, including reproductive studies
105 (Grawunder et al. 2015), transcriptomes (Sunagawa et al. 2009; Lehnert et al. 2012; Lehnert
106 et al. 2014) and an anemone genome sequence (Baumgarten et al. 2015). Prior work
107 evaluating multiple *E. diaphana* strains has shown variation in sexual reproduction
108 (Grawunder et al. 2015), Symbiodiniaceae specificity (Thornhill et al. 2013; Grawunder et al.

109 2015), and resistance to thermal stress (Bellis and Denver 2017; Cziesielski et al. 2018).
110 However, Australian contributions to these efforts have been hampered as researchers have
111 not had access to the established strains as import permits for alien species are difficult to
112 secure.

113 The aim of the present work is to add GBR representatives to the existing suite of *E.*
114 *diaphana* model strains. We describe the establishment and maintenance of four genotypes,
115 including their provenance, taxonomy, maintenance, histology, physiology, and
116 Symbiodiniaceae symbiont type. The results highlight characteristics that make GBR-sourced
117 *E. diaphana* a valuable extension to this coral model, such as the physiological and genetic
118 variability between genotypes, which is more representative of a global population. This
119 foundation information will be useful to international researchers interested in using the
120 GBR-sourced animals in their research and will give Australian researchers access to this
121 valuable model.

122 2 Methods

123 2.1 Anemone acquisition and husbandry

124 Several pieces of coral rubble bearing anemones were obtained from holding tanks in the
125 National Sea Simulator (SeaSim) at the Australian Institute of Marine Science and sent to
126 Swinburne University of Technology, Melbourne (SUT) in late 2014. Additional anemones
127 from the SeaSim were sent to the Marine Microbial Symbiont Facility (MMSF) at the
128 University of Melbourne (UoM) in early 2016. Most material in the SeaSim tanks originates
129 from the central GBR; therefore, this is the likely origin of the anemones. The SUT and UoM
130 populations were consolidated at MMSF in early 2017 where they were segregated according
131 to single polynucleotide polymorphism (SNP) analysis groupings (see below). Anemones
132 were grown in 4 L polycarbonate tanks in reverse osmosis (RO) water reconstituted Red Sea
133 Salt™ (RSS) at ~34 parts per thousand (ppt), and incubated without aeration or water flow at
134 26°C under lighting of 12-20 $\mu\text{mol photons m}^{-2} \text{s}^{-1}$ (light emitting diode - LED white light
135 array) on a 12h:12h light:dark cycle in a walk-in incubator. Anemones were fed *ad libitum*
136 with freshly hatched *Artemia salina* (brine shrimp, Salt Creek, UT, USA) nauplii twice
137 weekly. Tanks were cleaned each week after feeding by loosening algal debris with water
138 pressure applied through disposable plastic pipettes, removing algal biomass, and complete
139 water changes. When cleaning, ~25% of the anemones were cut into 2-6 fragments to
140 promote population expansion through regeneration of the tissue fragments into whole
141 anemones. Every third week, all anemones were transferred to clean tanks.

142 2.2 Anemone identity and genotyping

143 Anemone identity was determined by Sanger sequencing of the 18S rRNA gene. Genomic
144 DNA (gDNA) was extracted from six whole anemones following the protocol described by
145 Wilson et al. (2002), modified with a 15 min incubation in 180 μM lysozyme, and 30 s bead
146 beating at 30 Hz (Qiagen Tissue-Lyser II) with 100 mg of sterile glass beads (Sigma G8772).
147 The 18S rRNA genes were PCR amplified from all anemone samples using external
148 Actiniaria-specific 18S rRNA gene primers 18S_NA, 5'-
149 TAAGCACTTGTCTGTGAAACTGCGA-3' and 18S_NB, 5'-TAAGCACTTGT
150 CTGTGAAACTGCGA-3' (Grajales and Rodriguez 2016) with 0.5 U 2x Mango Mix
151 (Bioline), 2 μL of DNA template, 0.2 μM of each primer, and nuclease-free water up to 25
152 μL . PCR conditions consisted of initial denaturation at 94°C for 5 min, 35 cycles of 94°C for
153 45 s, 55°C for 45 s, and 72°C for 45 s followed by a final extension at 72°C for 5 min. PCR

154 products were purified with an ISOLATE II PCR and Gel Kit (Bioline, BIO-52059)
155 according to the manufacturers guidelines, and supplied to the Australian Genome Research
156 Facility (AGRF) for Sanger sequencing with the external primers and four internal primers:
157 18S_NL, 5'-AACAGCCCGGTCAGTAACACG-3', 18S_NC 5'-
158 AATAACAATACAGGGCTTTTCTAAGTC-3', 18S_NY 5'-
159 GCCTTCCTGACTTTGGTTGAA-3', and 18S_NO 5'-
160 AGTGTTATTGGATGACCTCTTTGGC-3'. The raw 18S reads were aligned in Geneious (v
161 10.0.4) (Kearse et al. 2012) to produce the near-complete 18S rRNA gene sequence, which
162 was evaluated by BLASTn (Altschul et al. 1990) to identify the anemones.

163 For genotyping, DNA was extracted as described above from 23 whole anemones or their
164 tentacles and sent to Diversity Arrays Technology Pty Ltd (Canberra, Australia) for DArT
165 next-generation sequencing (DArTseq). DArTseq combines complexity reduction and next
166 generation sequencing to generate genomic data with a balance of genome-wide
167 representation and coverage (Cruz et al. 2013). Complexity reduction was achieved by using
168 restriction endonucleases to target low-copy DNA regions. These regions were then
169 sequenced using Illumina HiSeq2500 (Illumina, USA) with an average read depth exceeding
170 20x. The data were processed by DArT Pty Ltd to remove poor quality sequences and to
171 ensure reliable assignment of sequences to samples. DArTsoft14 was then used to identify
172 SNPs at each locus as homozygous reference, homozygous alternate or heterozygous for each
173 individual (Melville et al. 2017). Monomorphic loci, loci with <100% reproducibility or
174 missing values were removed in the R package, dartR, to improve the quality of and reduce
175 linkage within the dataset; this reduced the dataset from 8288 loci to 1743 loci (R Core Team
176 2013; Gruber et al. 2017).

177 Euclidean distances between individual anemones, based on differences in the allele
178 frequencies at each of the SNP loci, were calculated from the reduced SNP dataset in dartR,
179 then viewed as a histogram and printed into a matrix in RStudio. Although the genetic distance
180 between individuals of the same genotype should be zero, small differences may occur due to
181 sequencing errors and somatic mutations. The genetic distance between individuals of different
182 genotypes will be larger than that within individuals. Therefore, the genetic distances among
183 individuals from several genotypes should form a bi- or multi-modal distribution; one peak
184 with a relatively small mean represents genetic distances between pairs of individuals of the
185 same genotype, another represents inter-genotypic distances with a larger mean. The inter-

186 genotypic distribution can be multi-modal because different pairs of genotypes can differ by
187 different amounts. Note that two samples from the same individual were genotyped to
188 determine methodological error rates and verify the baseline for clonality. A principal
189 coordinates analysis was performed and plotted in dartR to visualize the genotype assignments.

190 To compare the phylogenetic relationship of the GBR-sourced anemones with the previously
191 described clonal lines, we used a set of four *Exaiptasia*-specific inter-simple sequence repeat
192 (ISSR)-derived sequence characterized amplified region (SCAR) markers developed by
193 Thornhill et al. (2013) and an additional six *Exaiptasia*-specific gene loci (Bellis and Denver
194 2017). gDNA was extracted from five animals of each genotype, as described above, and
195 amplified with each of the four SCAR marker (3, 4, 5, and 7) and gene primer pairs
196 (Thornhill et al. 2013; Bellis and Denver 2017). PCR solutions for each marker contained
197 0.5U MyTaq HS Mix polymerase (Bioline), 1 μ L of DNA template, 0.4 μ M of each primer,
198 and nuclease-free water up to 25 μ L. Thermocycling consisted of an initial denaturation at
199 94°C for 1.5 min, 35 cycles of 94°C for 1 min, 56°C for 1 min, and 72 °C for 1.5 min
200 followed by a final extension at 72°C for 5 min. Amplified products were purified and
201 sequenced in forward and reverse directions at AGRF. Sequences were aligned and edited in
202 Geneious version 2019.2. Substantial non-specific binding of the SCAR marker 7 primers
203 generated unusable sequence data. Further, the forward and reverse sequences from two
204 anemone genotypes that were heterozygous for two or more indels at different points in the
205 sequences of SCAR markers 3 (anemone AIMS1) and 4 (anemones AIMS2-4) could not be
206 aligned and this prohibited the inclusion of those loci from analyses. Therefore, only
207 sequence data from SCAR marker 5 was used for phylogenetic analyses. For the six
208 *Exaiptasia*-specific gene loci, only AIPGENE19577, Atrophin-1-interacting protein 1 (AIP1)
209 contained heterozygous indels or non-specific binding of the forward primer.

210 For each genotype, the SCAR marker 5 sequences and each of the six *Exaiptasia*-specific
211 gene loci of the clonal replicates were aligned and a consensus sequence was generated. For
212 the SCAR marker, the consensus sequences were aligned with twelve reference sequences
213 from Thornhill et al. (2013) and three experimental anemone sequences (Grawunder et al.
214 2015), while the *Exaiptasia*-specific gene sequences were aligned with five reference
215 sequences from Bellis and Denver (2017). Each alignment was used to create a phylogenetic
216 tree using the Maximum Likelihood method and General Time Reversible model (Nei and
217 Kumar 2000) in MEGA X (Kumar et al. 2018). Topology, branch length, and substitution

218 rate were optimized, and branch support was estimated by bootstrap analysis of 1000
219 iterations.

220 2.3 GBR anemone gender determination

221 Over a period of two months, several anemone individuals from each genotype were reared to
222 a pedal disk diameter of ~7 mm. One animal per genotype was anesthetized in a 1:1 solution
223 of 0.37 M magnesium chloride and filter-sterilized RSS (fRSS) for 30 min, dissected and
224 viewed under a stereo microscope (Leica MZ8) to confirm the presence of gonads. When
225 gonads were observed, one animal per genotype was anesthetized as described above, fixed
226 in 4% paraformaldehyde in 1x PBS (pH 7.4) overnight, washed three times in 1x PBS and
227 processed by the Biomedical Histology Facility of The University of Melbourne. Samples
228 were embedded in paraffin and 7 µm transverse sections were cut (see supplemental
229 information Online Resource 1 for histological processing). Slides were stained with
230 hematoxylin and eosin (H&E) and viewed under a compound microscope (Leica DM6000B).

231 2.4 Symbiodiniaceae

232 The ITS2 region of Symbiodiniaceae gDNA was analyzed by metabarcoding to determine the
233 Symbiodiniaceae species associated with the GBR-sourced anemones. gDNA extracted from
234 three animals of each genotype, as described above, was amplified in triplicate with the ITS-
235 Dino (forward; 5'-
236 TCGTCGGCAGCGTCAGATGTGTATAAGAGACAGGTGAATTGCAGAACTCCGTG-
237 3') (Pochon et al. 2001) and its2rev2 (reverse; 5'-
238 GTCTCGTGGGCTCGGAGATGTGTATAAGAGACAGCCTCCGCTTACTTATATGCTT-
239 3') (Stat et al. 2009) primers modified with Illumina adapters. PCRs included 0.5 U MyTaq
240 HS Mix polymerase (Bioline), 1 µL of DNA template, 0.25 µM of each primer, and nuclease-
241 free water up to 20 µL. Thermocycling consisted of an initial denaturation at 95.0 °C for 3
242 min, 35 cycles at 95.0 °C, 55.0 °C and 72.0 °C for 15 sec each, and 1 cycle at 72 °C for 3
243 min. Library preparation on pooled triplicates and Illumina MiSeq sequencing (2x250 bp)
244 was performed by the Ramaciotti Centre for Genomics at the University of New South
245 Wales, Sydney. Raw, demultiplexed MiSeq read-pairs were joined in QIIME2 v2018.4.0
246 (Bolyen et al. 2018). Denoising, chimera checking, and trimming was performed in DADA2
247 (Callahan et al. 2016). The remaining sequences were clustered into operational taxonomic
248 units (OTUs) at 99% sequence similarity using closed-reference OTU picking in vsearch

249 (Rognes et al. 2016). A taxonomic database adapted from Arif et al. (2014) was used to seed
250 the OTU clusters and for taxonomic classification.

251 2.5 Anemone and Symbiodiniaceae physiological properties

252 Physiological assessments were performed on anemones maintained in a healthy, unbleached
253 state for over two years. Three of the four anemone genotypes named AIMS2, AIMS3, and
254 AIMS4, with oral disk diameters of 3-4 mm were transferred from the original holding tanks
255 in the walk-in incubator and randomly distributed between three replicate (by genotype) 250
256 mL glass culture containers containing RSS. Anemones of this size were chosen as they were
257 considered sexually immature (Muller-Parker et al. 1990; Grawunder et al. 2015) and
258 therefore variability in sexual development or gonadal reserves were unlikely to influence the
259 results. AIMS1 was excluded from long-term assessment as it had poor survival at densities
260 required for the analyses.

261 Glass culture containers were transferred from the walk-in incubator to experimental growth
262 chambers (Taiwan HiPoint Corporation model 740FHC) fitted with red, white, and infrared
263 LED lights. Initial light levels were set at $12 \mu\text{mol photons m}^{-2} \text{s}^{-1}$ (HiPoint HR-350 LED
264 meter) to correspond with the walk-in incubator conditions and ramped up to $28 \mu\text{mol}$
265 $\text{photons m}^{-2} \text{s}^{-1}$ over a period of 72 h on a 12 h:12 h light:dark cycle to approximate
266 experimental conditions reported in *E. diaphana* literature (Online Resource 2; Fransolet et
267 al. 2014; Hoadley and Warner 2017). While the commonly used *E. diaphana* strains (CC7,
268 H2, RS) are often maintained at $>50 \mu\text{mol photons m}^{-2} \text{s}^{-1}$ (pers. comm.), the GBR strains
269 appeared healthier, with extended bodies and open tentacles, at lower light intensities. The
270 anemones were maintained in RSS, fed *A. salina* nauplii and cleaned as described above. The
271 pH, salinity and temperature of the water and applied light levels were monitored thrice
272 weekly and were stable over time: 8.14 ± 0.02 , 35.0 ± 0.04 ppt, $25.77 \pm 0.07^\circ\text{C}$ and 28.08 ± 0.12
273 $\mu\text{mol photons m}^{-2} \text{s}^{-1}$, respectively. Culture containers were placed on a single incubator shelf
274 and randomly rearranged after each clean to minimize confounding by position.

275 The maximum dark adapted quantum yield (Fv/Fm) of photosystem II (PSII) of *in hospite*
276 Symbiodiniaceae provides an indication of photosynthetic performance and is useful as a bio-
277 monitoring tool (Howe et al. 2017). Fv/Fm is measured as the difference in fluorescence
278 produced by PSII reaction centers when either saturated by intense light (Fm) or in the
279 absence of light (Fo), versus Fm (i.e. $(Fm - Fo)/Fm$, or Fv/Fm). Symbiodiniaceae Fv/Fm was

280 measured weekly over nine weeks for each culture container after 4 hr into the incubator light
281 cycle and 30 mins dark adaption using imaging pulse amplitude modulated (iPAM)
282 fluorometry (IMAG-MAX/L, Waltz, Germany). Settings for all measurements were:
283 saturating pulse intensity 8, measuring light intensity 2 with frequency 1, actinic light
284 intensity 3, damping 2, gain 2. Average Fv/Fm values for each dish were calculated from
285 readings taken on three to five anemones (Online Resource 3).

286 Anemones from each culture container were individually homogenized in a sterile glass
287 homogenizer in 1 mL fRSS, and 100 μ L of homogenate was collected and stored at -20°C
288 for total protein measurement. The remaining 900 μ L of homogenate was centrifuged at 5000
289 g for 5 min at 4°C to pellet the Symbiodiniaceae while leaving the anemone cells in
290 suspension. A volume of 100 μ L of supernatant was collected and stored at -20°C for host
291 protein measurement. The pelleted Symbiodiniaceae were twice washed with 500 μ L fRSS
292 and centrifuged at 5000 g for 5 min at 4°C , and the final pellet resuspended in 500 μ L fRSS
293 and stored at -20°C for Symbiodiniaceae counts. Triplicate cell counts (cells mL^{-1}) were
294 completed within 48 hrs of sample collection on a Countess II FL automated cell counter
295 (Life Technologies) and normalized to host protein (mg mL^{-1}). This process was repeated 15
296 times over the course of nine weeks for a total of 45 replicates per genotype.

297 Samples for protein analysis stored at -20°C (see above) were used within one month of
298 collection to determine total and host protein (mg mL^{-1}) by the Bradford assay (Bradford
299 1976) against bovine serum albumin standards (Bio-Rad 500-0207). Readings were taken at
300 595 nm (EnSpire microplate reader MLD2300).

301 Fv/Fm values and Symbiodiniaceae cell densities were assessed for genotype-specific
302 responses. All variables were tested for normality and homoscedasticity prior to parametric
303 analyses, which were completed in R (v 3.6.0). Genotypic responses of Fv/Fm were
304 compared using a linear model in the R package nlme (Pinheiro et al. 2017) to evaluate
305 independent and interaction relationships between the factors of genotype and time. F-
306 statistics were obtained using the analysis of variance (ANOVA) function, nlme, and
307 pairwise *post hoc* analyses were performed using the glht function in the R package
308 multcomp (Hothorn et al. 2016) with Tukey's correction for multiple comparisons.
309 Symbiodiniaceae cell densities were pooled across time by genotype and analyzed with a
310 one-way ANOVA with a *post hoc* Tukey test to determine pairwise significance.

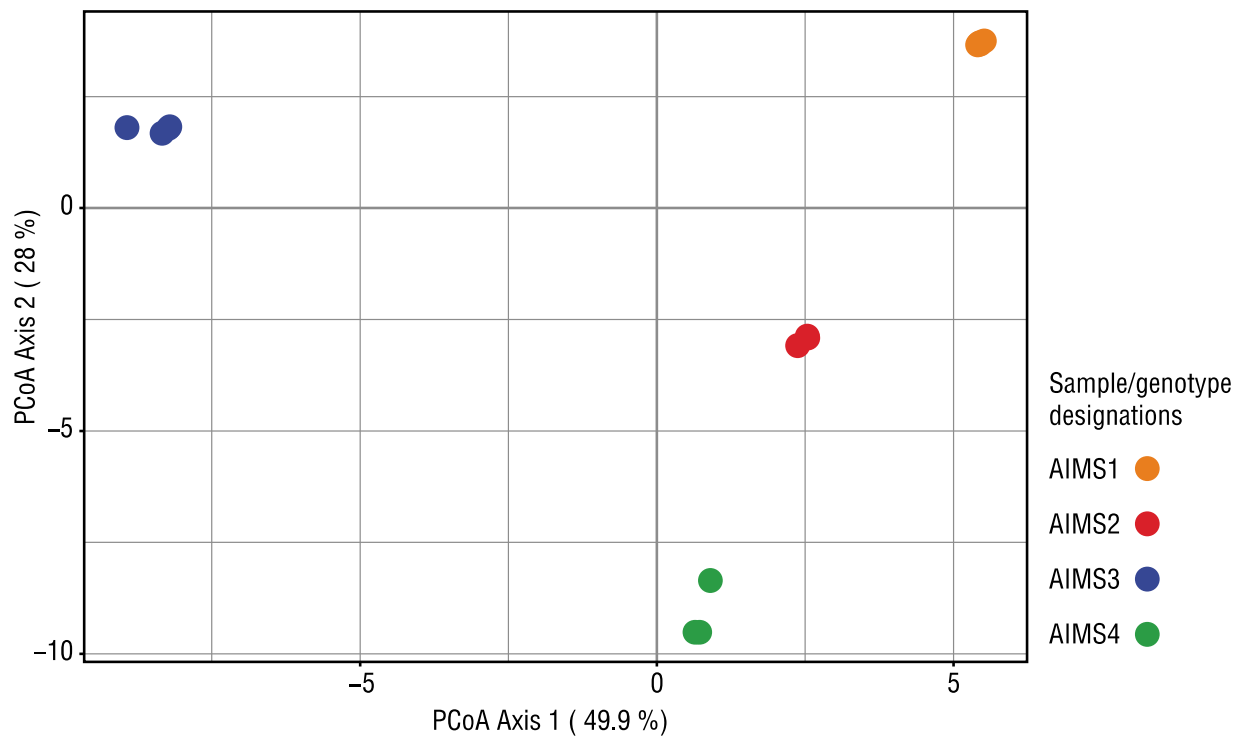
311 **Results and Discussion**

312 3.1 Anemones

313 The assembled 18S rRNA gene sequences of two genotypes (AIMS2 and AIMS4) covered
314 1591 and 1594 bp, respectively, with two mismatches between the sequences. BLASTn
315 against the NCBI database identified the samples as either *Aiptasia pulchella* or *Exaiptasia*
316 *pallida*. *A. pulchella* has been synonymised with *E. pallida* (Grajales and Rodríguez, 2014).
317 However, since *E. diaphana* has precedence (ICZN 2017), all samples were designated *E.*
318 *diaphana*.

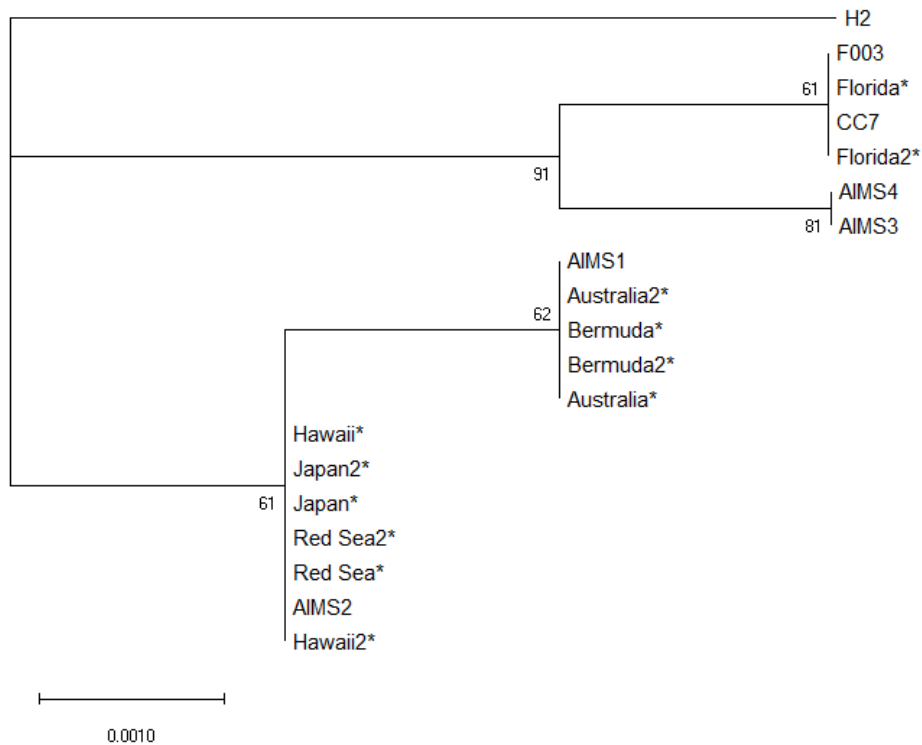
319 Four SNP genotypes of *E. diaphana*, which were of GBR-origin but AIMS-sourced, were
320 identified and designated AIMS1, AIMS2, AIMS3 and AIMS4 (Fig. 1). The clonal
321 distribution of Euclidean distances was identified (range of 0-9.61) and pairs of individuals
322 with Euclidean distances within this distribution were inferred to have the same genotype
323 (Online Resource 3-4). The Euclidean distance between the originally named Ed.11a and
324 Ed.11b (replicates from the same individual; assigned AIMS3) is in the upper percentiles of
325 the defined clonal distribution, confirming this cut-off is valid.

326 Using phylogenetic analysis with our data, previously described SCAR marker 5, and the
327 *Exaiptasia*-specific gene sequence data (Thornhill et al. 2013; Grawunder et al. 2015; Bellis
328 and Denver 2017), we placed the GBR anemones into a phylogeographical context. The
329 alignment of SCAR5 sequences was 706 bp long and contained 19 variable nucleotide
330 positions (Fig. 2), while the concatenated *Exaiptasia*-specific gene sequences were 3276 bp
331 long with 92 variable nucleotide positions (Fig. 3).



332

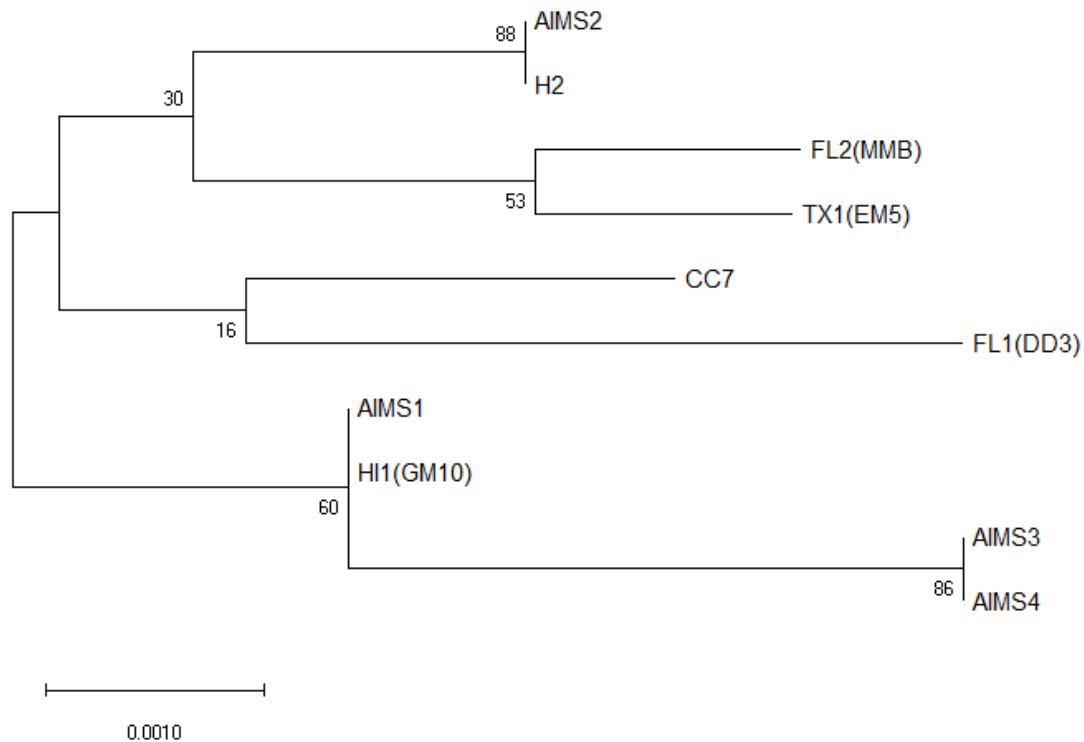
333 **Figure 1:** PCoA ordination of *Exaiptasia diaphana* genotypes based on Euclidean genetic distance measurements
334 of SNP data using allele frequencies within individuals to calculate genetic distance between them (AIMS1, n=8;
335 AIMS2, n=5, AIMS3, n=7; AIMS4, n=3). Individuals of the same genotype may overlap in the plot due to their
336 high similarity.



337

338 **Figure 2:** The phylogenetic relationships of the four GBR *E. diaphana* compared to other conspecific anemones
339 sampled across the globe inferred from SCAR marker 5 using the Maximum Likelihood method and General
340 Time Reversible model (Nei and Kumar 2000). The tree with the highest log likelihood is shown with bootstrap
341 values next to the nodes. Initial trees for the heuristic search were obtained automatically by applying the
342 Maximum Parsimony method. The tree is drawn to scale, with branch lengths measured in the number of
343 substitutions per site. This analysis involved 19 *E. diaphana* sequences and 706 nucleotide positions were
344 included. Sequences were from our *E. diaphana* genotypes (AIMS1-4), globally distributed *E. diaphana* from

345 Thornhill et al. (2013), indicated with an asterisk, and from experimental genotypes CC7, H2, and F003
346 (Grawunder et al. 2015).



347

348 **Figure 3:** The phylogenetic relationships of the four GBR *E. diaphana* (AIMS1-4) compared to other
349 experimental anemones using the Maximum Likelihood method and General Time Reversible model (Nei and
350 Kumar 2000) on six concatenated *Exaiptasia*-specific gene sequences (Bellis and Denver 2017). Data from Bellis
351 and Denver (2017) was downloaded from GenBank (accession numbers KU847812-KU847847); tree branches
352 are named as strain name followed by the alternative strain name in parentheses. Bootstrap values are shown next
353 to the nodes. Initial trees for the heuristic search were obtained automatically by applying the Maximum
354 Parsimony method. The tree is drawn to scale, with branch lengths measured in the number of substitutions per
355 site. This analysis involved 10 *E. diaphana* sequences and 3267 nucleotide positions were included.

356 Based on SCAR marker data, *E. diaphana* is regarded as a single pan-global species with two
357 distinct genetic lineages: one from the USA Atlantic coast, and a second consisting of all other
358 *E. diaphana* worldwide (Thornhill et al. 2013). The SCAR5 allele sequenced for genotype
359 AIMS1 is identical with that from anemones originally collected off Heron Island, Australia
360 and Bermuda, while that of AIMS2 is nearly identical to (two base pair differences, both with
361 an ambiguous base) samples from Hawaii, Japan and the Red Sea. AIMS3 and AIMS4 are
362 most closely related to anemones from Florida and North Carolina, USA and are identical to
363 one another in this region.

364 Similar to Bellis and Denver (2017), our data from the *Exaiptasia*-specific gene sequences
365 (Fig. 3) show that, while anemone strains are genetically distinct, there is not a strong

366 phylogenetic separation between individuals collected from distant geographic locations.
367 Again, AIMS1-4 show genetic variation, with AIMS1 and AIMS2 clustering with anemone
368 strains originating from Coconut Island, Hawaii, USA which were collected independently in
369 1979 and early 2000's, respectively. Corresponding with the SCAR5 loci data, AIMS3-4 have
370 near identical sequences in the sequenced regions (differences at two heterozygous sites).
371 Because the available data for SCAR5 and the *Exaiptasia*-specific gene targets are not from all
372 the same individuals, with the exception of CC7 and H2, comparing between the two is not
373 feasible. However, given the larger number of alignment positions and variable sites in the
374 gene regions with better PCR results, we suggest that researchers use the primers presented in
375 Bellis and Denver (2017) for future comparisons between *E. diaphana* used in experiments.
376 The diversity that is revealed by whole genome SNP analysis (Fig. 1) is hidden with these six
377 *Exaiptasia*-specific gene sequences, suggesting that there are more informative loci not yet
378 published for *E. diaphana* genotyping.

379 There are several possible explanations for the AIMS1-4 anemones to be spread throughout
380 the phylogenetic trees. First, due to small sample sizes at all sampling locations, only a subset
381 of the alleles have been sampled and location-specific alleles may have been missed. Second,
382 it is conceivable that the GBR is the source of all other *E. diaphana* populations and founder
383 effects mean that other geographic locations have *E. diaphana* that represent only some of the
384 diversity. Third, it is possible that the GBR *E. diaphana* was a distinct lineage and the GBR
385 has since been invaded by *E. diaphana* from other lineages, or the GBR lineage has been
386 introduced elsewhere. Introductions over such vast spatial scales may have occurred via ship
387 ballast water or attached to ships hulls in fouling biomass, which is notorious for transporting
388 marine life and introducing invasive animals and plants, or via the aquarium trade or marine
389 farms. Irrespective of the cause, the genetic variation across the four GBR genotypes is more
390 representative of global diversity than a single localized population. Because strain-specific
391 responses to environmental variables have been observed among *E. diaphana* strains (Bellis
392 and Denver 2017; Czielski et al. 2018) it is critical to conduct experiments, such as those
393 regarding climate change and symbiosis, with a diverse set of individuals, much like the
394 diversity presented by the GBR-sourced *E. diaphana*.

395 3.2 Symbiosis with Symbiodiniaceae

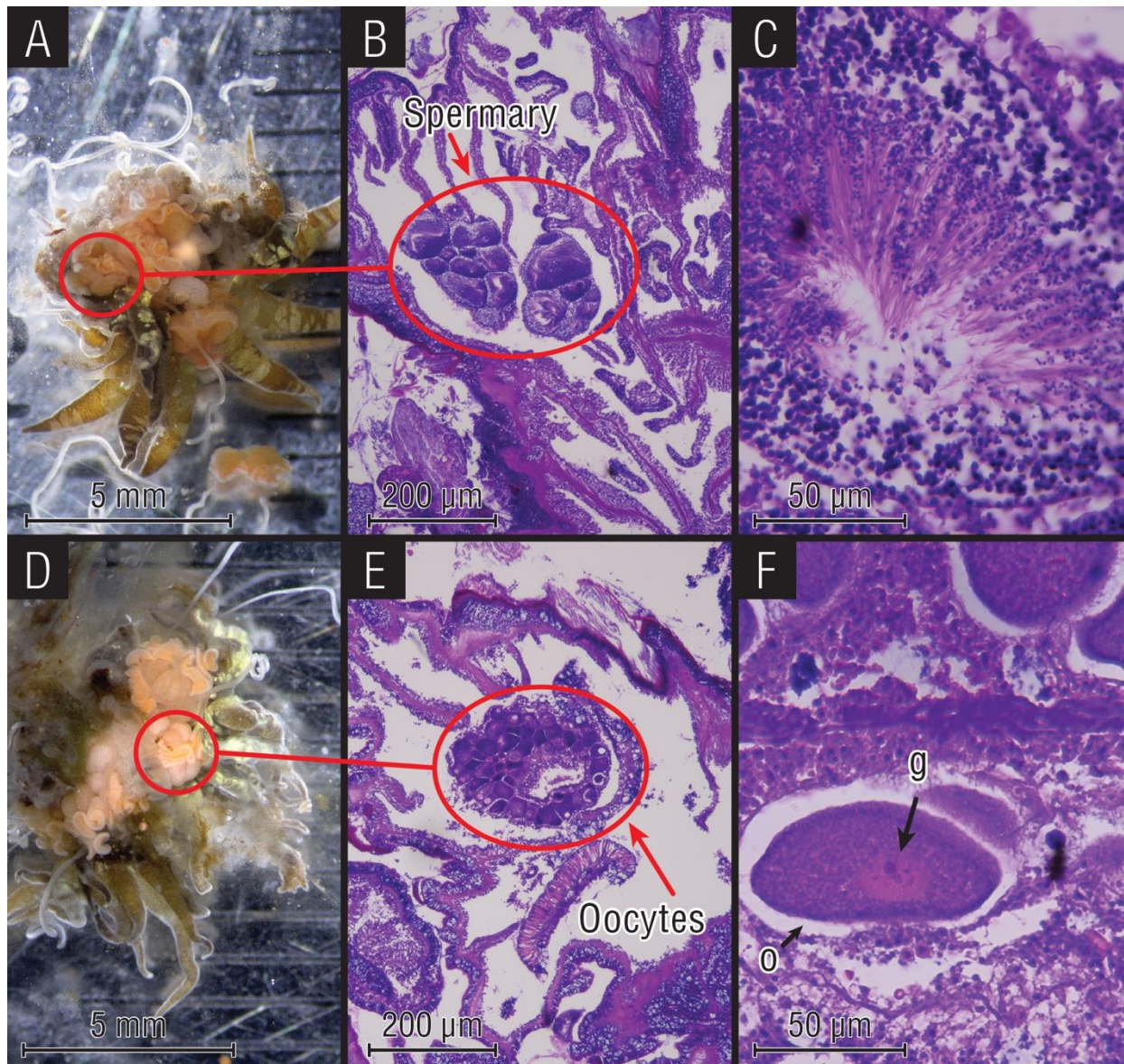
396 According to a global survey by Thornhill et al. (2013), Pacific Ocean *E. diaphana* (e.g., H2)
397 associate exclusively with the Symbiodiniaceae species *Breviolum minutum* (formerly ITS2

398 type *Symbiodinium* Clade B, sub-clade B1 (LaJeunesse et al. 2018)). Symbiodiniaceae
399 sequences from the four GBR *E. diaphana* genotypes were almost exclusively *Breviolum*
400 *minutum* (>99.6%), thus concurring with Thornhill et al. (2013). Two as-yet unnamed species
401 of *Breviolum* (previously known as *Symbiodinium* sub-clades B1i and B1L (LaJeunesse et al.
402 2018)) were also identified in *E. diaphana*. Their very low relative abundance suggests they
403 are either intragenomic variants or rare strains.

404 Stable endosymbiotic relationships between corals and Symbiodiniaceae are vital for
405 sustaining coral reef ecosystems; this symbiotic relationship is the focus of much coral reef
406 research. Interestingly, while the GBR anemones are genetically diverse, all host *B. minutum*
407 as their sole Symbiodiniaceae. Given this, we may be able to investigate the symbiotic
408 mechanisms of the host-algal relationship and answer questions about this symbiosis that are
409 not restricted by anemone strain.

410 3.3 Sex of *E. diaphana*

411 *E. diaphana* lacks obvious gender defining morphological features, but gonad development is
412 related to size (Chen et al. 2008). Partially developed oocytes with germinal vesicles (*i.e.*, the
413 nucleus of an oocyte arrested in prophase of meiosis I) were observed in histological slides in
414 animals of AIMS1, AIMS3 and AIMS4 and Stage V spermaries were observed in AIMS2 (Fig.
415 4). In Stage V, the spermary is made up of a mass of spermatozoa with their tails facing in the
416 same direction. In this advanced stage the spermatozoa are capable of fertilization (Fadlallah
417 and Pearse 1982; Goffredo et al. 2012). While most AIMS1 anemones grew to only 5 mm in
418 pedal disk diameter, gonad development was still observed. Differences between male and
419 female gonads were present but were macroscopically cryptic. Male gonads have been
420 observed to be smaller and lighter colored than female gonads in *E. diaphana* (Grawunder et
421 al. 2015), and this was also the case in the GBR-sourced females (AIMS1, AIMS3 and AIMS4)
422 and male (AIMS2) *E. diaphana*.

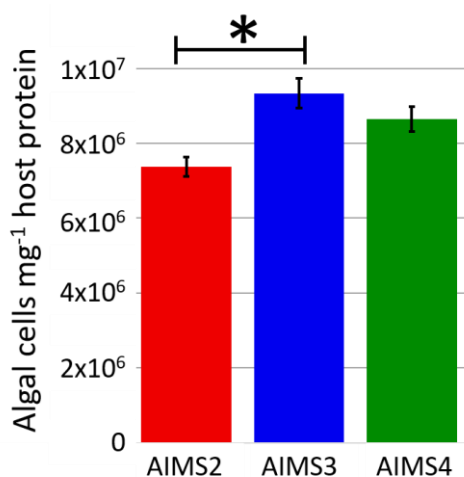


423

424 **Figure 4:** (A) Dissected male anemone with developing gonads (AIMS2, ~1 cm pedal disk diameter); (B) H&E
425 stained tissue section, with stage 5 spermary; (C) Increased magnification of stage 5 spermary; (D) dissected
426 female anemone with developed gonads (AIMS4, ~1 cm pedal disk diameter); (E) H&E stained tissue section
427 with oocytes; (F) increased magnification of female gonad with developing oocyte (o) and germinal vesicle (g).

428 3.4 *E. diaphana* and Symbiodiniaceae Physiology

429 Throughout the nine-week evaluation period all *E. diaphana* maintained a healthy
430 appearance, including *in hospite* Symbiodiniaceae, tentacle extension, active feeding of *A.*
431 *salina* nauplii and asexual propagation. Average Symbiodiniaceae cell densities (normalized
432 to host protein) were significantly different between genotypes (one-way ANOVA
433 ($F_{(3,200)}=3.985$, $p=0.00872$; Fig. 5; Online Resource 6). All anemones hosted $\sim 10^6$
434 Symbiodiniaceae cells mg^{-1} host protein, which is comparable to densities reported for other
435 lab cultured model *E. diaphana* systems (Hoadley et al. 2015; Hawkins et al. 2016b;
436 Radecker et al. 2018) and is similar to Symbiodiniaceae cell densities found in scleractinian
437 corals (Cunning and Baker 2014; Ziegler et al. 2015; Kenkel and Bay 2018). The only
438 statistically significant difference observed was the lower Symbiodiniaceae cell density of
439 AIMS2 (mean \pm SE; $7.17 \times 10^6 \pm 2.73 \times 10^5$ per mg host protein, $n=66$) compared to AIMS3
440 (mean \pm SE; $8.46 \times 10^6 \pm 2.96 \times 10^5$ per mg host protein, $n=66$) (Fig. 5).



441

442 **Figure 5:** Mean \pm 1SEM Symbiodiniaceae cells mg^{-1} host protein for GBR *E. diaphana* genotypes AIMS2-4.
443 Seventy-five AIMS2-4 anemones were collected over a period of nine weeks. Asterisk indicates significant
444 difference, $p < 0.05$.

445 All genotypes experienced a nearly identical drop in Fv/Fm after the light intensity was
446 increased from 12 to 28 $\mu\text{mol photons m}^{-2} \text{s}^{-1}$, from an average of 0.53 on day 0, to an
447 average of 0.40 by day 21 (Online Resource 7; Fig. 6). However, by day 36 the Fv/Fm values
448 had returned to initial levels.

449 Changes in environmental variables, such as light intensity, are known to influence
450 photobiological behavior of Symbiodiniaceae (Wangpraseurt et al. 2014; Hoadley and

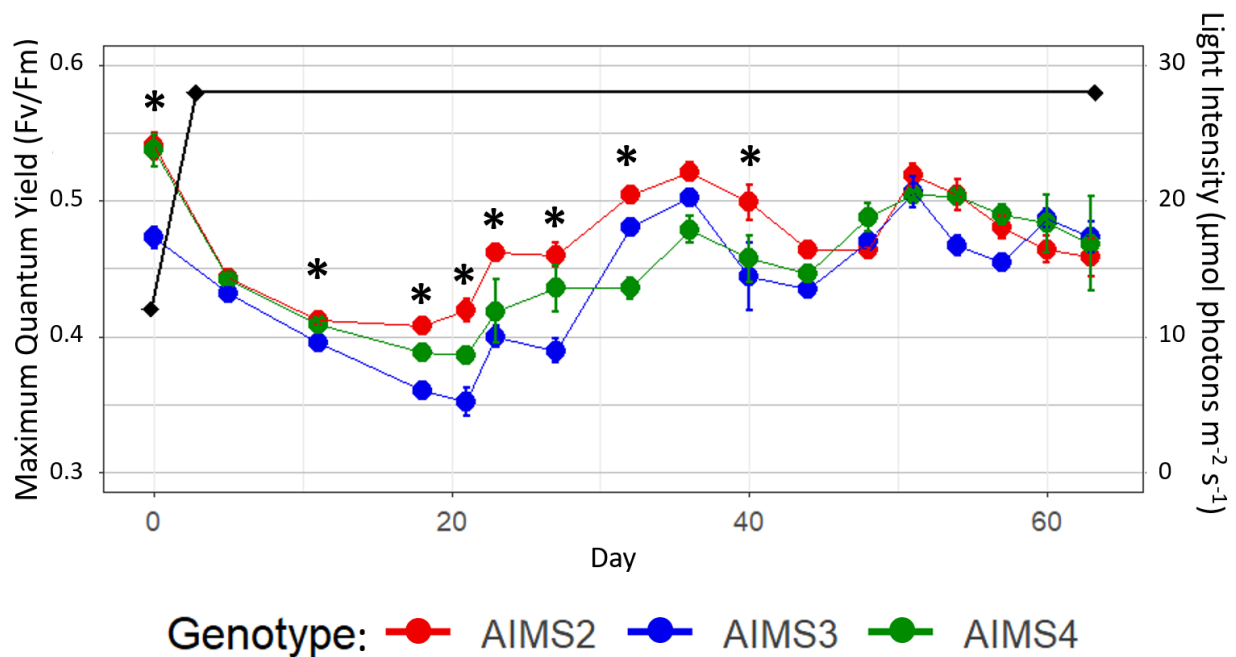
451 Warner 2017). A change in light intensity can alter photosynthetic efficiency as measured by
452 Fv/Fm (Hoadley and Warner 2017). GBR anemone genotypes AIMS2, AIMS3 and AIMS4
453 took 36 d to recover from this environmental change and return to photosynthetic efficiencies
454 recorded at $12 \mu\text{mol photons m}^{-2} \text{ s}^{-1}$. Such information is critical for planning and conducting
455 symbiosis studies. Most of the statistical differences between the genotypes occurred between
456 days 19-28 (Online Resource 8) when Fv/Fm was lowest. Once acclimated at day 36, average
457 Fv/Fm values for all genotypes were not significantly different (mean \pm SE; 0.479 ± 0.003 ,
458 $n=80$), except for day 40 where the Fv/Fm of AIMS2 was significantly higher than AIMS3
459 ($p=0.0068$).

460 As all the GBR-sourced anemones harbour *Breviolum minutum* as their homologous
461 symbiont type, it is not unexpected that the different genotypes would have similar maximum
462 Fv/Fm values. Furthermore, similar Fv/Fm values have been reported for other anemones
463 hosting homologous *B. minutum* (Hawkins et al. 2016b; Hillyer et al. 2017). However, it is
464 noteworthy that AIMS2 is not only able to recover its photosynthetic efficiency quicker from
465 changing light levels with a milder dip in Fv/Fm values (Fig. 6), but also hosts significantly
466 fewer Symbiodiniaceae cells mg^{-1} host protein compared to AIMS3 (Fig. 5). Reductions in
467 the maximum quantum yield of photosystem II (PSII) (Fv/Fm) is observed in the early phases
468 of natural bleaching events (Gates et al. 1992; Franklin et al. 2004) and the ability of AIMS2
469 to maintain a higher efficiency of PSII photochemistry during changing environmental
470 conditions could translate into higher thermal tolerance (Suggett et al. 2008; Ragni et al.
471 2010; Goyen et al. 2017).

472 These individuals are genetically diverse based on SNP genotyping (Fig. 1) and phylogenetic
473 analysis (Fig. 2-3); the phenotypic feature of AIMS2 being more robust to increasing light
474 levels compared to AIMS3 and AIMS4 could be a host genotypic effect. There is evidence
475 that genetic variation of *E. diaphana* may influence holobiont response to heat stress, though
476 this hypothesis has only been tested on anemone strains hosting different Symbiodiniaceae
477 species (Bellis and Denver 2017; Cziesielski et al. 2018) or after experimentally bleaching
478 anemones and inoculating with new heterologous algal cells (Perez et al. 2001). As we have
479 four GBR-sourced *E. diaphana* genotypes with inherent genetic variability and all contain *B.*
480 *minutum* as their homologous symbiont, we will be able to explore the roles of host and
481 symbiont in the bleaching response.

482 An alternative possibility is that the GBR anemones' Symbiodiniaceae communities
483 comprise diversity that may be hidden under the resolution of the ITS2 sequences we used in
484 this experiment, which are driving the differences in photosynthetic efficiency. Distinct
485 strains of a given Symbiodiniaceae species can have different susceptibilities to thermal
486 stress (Ragni et al. 2010; Howells et al. 2012; Hawkins et al. 2016a), with evidence that these
487 variations in thermal optima can drive host-Symbiodiniaceae interactions (Hawkins et al.
488 2016a). Thus, varying rates of recovery of Fv/Fm among Symbiodiniaceae strains (Fig. 6)
489 could provide a mechanism for the emergence of novel and potentially resilient cnidarian-
490 Symbiodiniaceae associations in a rapidly warming environment.

491 Another explanation for the physiological differences between AIMS2 and AIMS3 (Fig. 5) is
492 through algal cell density moderation by the host. It is thought that the coral host controls
493 Symbiodiniaceae densities through nitrogen limitation (Falkowski et al. 1993), although the
494 mechanisms are not well understood (Davy et al. 2012). During temperature stress, higher
495 densities of Symbiodiniaceae have been implicated in increasing the susceptibility of corals
496 to bleaching, potentially as a result of the higher reactive oxygen species production relative
497 to corals' antioxidant capacity (Cunning and Baker 2012). Altogether, our data suggest that
498 AIMS2, which hosted fewer algal symbionts and recovered from increased light conditions
499 faster than AIMS3, may be more resilient to thermal stress, while AIMS3 could be more
500 susceptible to bleaching with AIMS4 as an intermediate.



501

502 **Figure 6:** Fv/Fm measurements for anemones AIMS2, AIMS3 and AIMS4 over a 63-day period. Anemones
503 were initially exposed to light levels (black line) of $12 \mu\text{mol photons m}^{-2} \text{s}^{-1}$ (12:12 light:dark cycle), which were
504 then increased to $28 \mu\text{mol photons m}^{-2} \text{s}^{-1}$ over a 72 h period. Day 0 marks the start of light ramping. The
505 anemones took ~35 d to recover their maximum quantum yield due to the increase in light exposure although
506 Symbiodiniaceae densities remained largely constant. Asterisks indicate significant differences in pairwise
507 comparisons between genotypes at given time points (Online Resource 8)

508 4 Conclusions and Future Directions

509 The study of *E. diaphana* anemones of GBR origin described here provide further
510 information on phenotypic and genetic variation within this species and complements data on
511 the more widely used *E. diaphana* strains CC7 and H2. The four genotypes in our collections
512 capture a level of genetic diversity previously observed in animals from different oceans and
513 are therefore a hugely valuable addition to the model collections. Knowledge of their
514 characteristics enhances and broadens the potential of this model system for climate change
515 research in corals, particularly, but not exclusively, for Australian researchers. We propose
516 future research on this collection should focus on characterization of associated prokaryotes
517 to explore the value of these animals as models for coral-prokaryote symbiotic interactions.
518 Future research in cnidarian-prokaryotic interactions would be enhanced by the development
519 of axenic (germ-free) or gnotobiotic (with a known microbial community) *E. diaphana*
520 cultures. They could be used to test the influence of native and non-native microbiota on
521 holobiont performance, and the ability of probiotic inocula to support animal health during
522 stress (Alagely et al. 2011; Damjanovic et al. 2017; Rosado et al. 2018).

523 5 Acknowledgments

524 This research was funded by Australian Research Council Discovery Project grants
525 DP160101468 (to MJHvO and LLB) and DP160101539 (to GIM and MJHvO). We thank
526 Lesa Peplow for facilitating transport of the initial anemone cultures from AIMS to SUT and
527 UoM and Rebecca Alfred from SUT for initial anemone culture maintenance. We
528 acknowledge Anton Cozijnsen, Keren Maor-Landaw, Samantha Girvan, Ruby Vanstone and
529 Gabriela Rodriguez from University of Melbourne for assisting with anemone husbandry and
530 Laura Leone, Lisa Foster, and Lona Dinha from the Melbourne Histology Platform for
531 histological sample preparation and sectioning. SCAR marker reference sequences were
532 provided by Dan Thornhill and Liz Hambleton (AG Guse Lab, Centre for Organismal Studies
533 (COS), Universität Heidelberg). MJHvO acknowledges Australian Research Council
534 Laureate Fellowship FL180100036.

- 535 Alagely A, Krediet CJ, Ritchie KB, Teplitski M (2011) Signaling-mediated cross-talk
536 modulates swarming and biofilm formation in a coral pathogen *Serratia marcescens*
537 *ISME J* 5:1609-1620 doi:10.1038/ismej.2011.45
- 538 Altschul SF, Gish W, Miller W, Myers EW, Lipman DJ (1990) Basic local alignment search
539 tool *Journal of molecular biology* 215:403-410 doi:10.1016/s0022-2836(05)80360-2
- 540 Arif C et al. (2014) Assessing Symbiodinium diversity in scleractinian corals via next-
541 generation sequencing-based genotyping of the ITS2 rDNA region *Mol Ecol* 23:4418-
542 4433 doi:10.1111/mec.12869
- 543 Baird AH, Bhagooli R, Ralph PJ, Takahashi S (2009) Coral bleaching: the role of the host
544 *Trends Ecol Evol* 24:16-20 doi:10.1016/j.tree.2008.09.005
- 545 Baumgarten S et al. (2015) The genome of *Aiptasia*, a sea anemone model for coral
546 symbiosis *Proc Natl Acad Sci U S A* 112:11893-11898
547 doi:10.1073/pnas.1513318112
- 548 Belda-Baillie CA, Baillie BK, Maruyama T (2002) Specificity of a model cnidarian-
549 dinoflagellate symbiosis *Biol Bull* 202:74-85 doi:10.2307/1543224
- 550 Bellis ES, Denver DR (2017) Natural Variation in Responses to Acute Heat and Cold Stress
551 in a Sea Anemone Model System for Coral Bleaching *Biol Bull* 233:168-181
552 doi:10.1086/694890
- 553 Blanquet R, Lenhoff HM (1966) A disulfide-linked collagenous protein of nematocyst
554 capsules *Science* 154:152-153
- 555 Bolyen E et al. (2018) QIIME 2: Reproducible, interactive, scalable, and extensible
556 microbiome data science. *PeerJ Preprints*,
- 557 Bradford MM (1976) A rapid and sensitive method for the quantitation of microgram
558 quantities of protein utilizing the principle of protein-dye binding *Analytical*
559 *biochemistry* 72:248-254
- 560 Bucher M, Wolfowicz I, Voss PA, Hambleton EA, Guse A (2016) Development and
561 Symbiosis Establishment in the Cnidarian Endosymbiosis Model *Aiptasia* sp *Sci Rep*
562 6:19867 doi:10.1038/srep19867
- 563 Callahan BJ, McMurdie PJ, Rosen MJ, Han AW, Johnson AJA, Holmes SP (2016) DADA2:
564 high-resolution sample inference from Illumina amplicon data *Nature methods* 13:581
- 565 Carlisle JF, Murphy GK, Roark AM (2017) Body size and symbiotic status influence gonad
566 development in *Aiptasia pallida* anemones *Symbiosis* 71:121-127
567 doi:10.1007/s13199-016-0456-1
- 568 Chen C, Soong K, Chen CA (2008) The smallest oocytes among broadcast-spawning
569 actinarians and a unique lunar reproductive cycle in a unisexual population of the
570 sea anemone, *Aiptasia pulchella* (Anthozoa : Actiniaria) *Zool Stud* 47:37-45
- 571 Cruz VM, Kilian A, Dierig DA (2013) Development of DArT marker platforms and genetic
572 diversity assessment of the U.S. collection of the new oilseed crop *Lesquerella* and
573 related species *PLoS One* 8:e64062 doi:10.1371/journal.pone.0064062
- 574 Cuning R, Baker AC (2012) Excess algal symbionts increase the susceptibility of reef
575 corals to bleaching *Nature Climate Change* 3:259-262 doi:10.1038/nclimate1711
- 576 Cuning R, Baker AC (2014) Not just who, but how many: the importance of partner
577 abundance in reef coral symbioses *Front Microbiol* 5:400
578 doi:10.3389/fmicb.2014.00400
- 579 Cziesielski MJ, Liew YJ, Cui G, Schmidt-Roach S, Campana S, Maronedze C, Aranda M
580 (2018) Multi-omics analysis of thermal stress response in a zooxanthellate cnidarian
581 reveals the importance of associating with thermotolerant symbionts *Proc Biol Sci*
582 285 doi:10.1098/rspb.2017.2654
- 583 Damjanovic K, Blackall LL, Webster NS, van Oppen MJH (2017) The contribution of
584 microbial biotechnology to mitigating coral reef degradation *Microbial biotechnology*
585 10:1236-1243 doi:10.1111/1751-7915.12769
- 586 Davis RH (2004) The age of model organisms *Nature Reviews Genetics* 5:69
587 doi:10.1038/nrg1250
- 588 Davy SK, Allemand D, Weis VM (2012) Cell biology of cnidarian-dinoflagellate symbiosis
589 *Microbiol Mol Biol Rev* 76:229-261 doi:10.1128/MMBR.05014-11

- 590 De'ath G, Fabricius KE, Sweatman H, Puotinen M (2012) The 27-year decline of coral cover
591 on the Great Barrier Reef and its causes Proc Natl Acad Sci U S A 109:17995-17999
592 doi:10.1073/pnas.1208909109
- 593 Duckworth CG, Picariello CR, Thomason RK, Patel KS, Bielmyer-Fraser GK (2017)
594 Responses of the sea anemone, *Exaiptasia pallida*, to ocean acidification conditions
595 and zinc or nickel exposure Aquat Toxicol 182:120-128
596 doi:10.1016/j.aquatox.2016.11.014
- 597 Eakin CM et al. (2016) Global Coral Bleaching 2014-2017 Status and an Appeal for
598 Observations Reef Encounter 31:20-26
- 599 Fabricius K, De'ath G, McCook L, Turak E, Williams DM (2005) Changes in algal, coral and
600 fish assemblages along water quality gradients on the inshore Great Barrier Reef
601 Marine pollution bulletin 51:384-398
- 602 Fadlallah Y, Pearse J (1982) Sexual reproduction in solitary corals: overlapping oogenic and
603 brooding cycles, and benthic planulas in *Balanophyllia elegans* Marine Biology
604 71:223-231
- 605 Falkowski PG, Dubinsky Z, Muscatine L, McCloskey L (1993) Population-Control in
606 Symbiotic Corals Bioscience 43:606-611 doi:Doi 10.2307/1312147
- 607 Franklin DJ, Hoegh-Guldberg O, Jones R, Berges JA (2004) Cell death and degeneration in
608 the symbiotic dinoflagellates of the coral *Stylophora pistillata* during bleaching Marine
609 Ecology Progress Series 272:117-130
- 610 Fransolet D, Roberty S, Plumier J-C (2014) Impairment of symbiont photosynthesis
611 increases host cell proliferation in the epidermis of the sea anemone *Aiptasia pallida*
612 Marine Biology 161:1735-1743 doi:10.1007/s00227-014-2455-1
- 613 Gates RD, Baghdasarian G, Muscatine L (1992) Temperature stress causes host cell
614 detachment in symbiotic cnidarians: implications for coral bleaching The Biological
615 Bulletin 182:324-332
- 616 Goffredo S et al. (2012) Unusual pattern of embryogenesis of *Caryophyllia inornata*
617 (scleractinia, caryophylliidae) in the mediterranean sea: Maybe agamic reproduction?
618 Journal of morphology 273:943-956
- 619 Goyen S, Pernice M, Szabó M, Warner ME, Ralph PJ, Suggett DJ (2017) A molecular
620 physiology basis for functional diversity of hydrogen peroxide production amongst
621 *Symbiodinium* spp.(Dinophyceae) Marine biology 164:46
- 622 Grajales A, Rodriguez E (2014) Morphological revision of the genus *Aiptasia* and the family
623 *Aiptasiidae* (Cnidaria, Actiniaria, Metridioidea) Zootaxa 3826:55-100
624 doi:10.11646/zootaxa.3826.1.2
- 625 Grajales A, Rodriguez E (2016) Elucidating the evolutionary relationships of the *Aiptasiidae*,
626 a widespread cnidarian-dinoflagellate model system (Cnidaria: Anthozoa: Actiniaria:
627 Metridioidea) Mol Phylogenet Evol 94:252-263 doi:10.1016/j.ympev.2015.09.004
- 628 Grawunder D, Hambleton EA, Bucher M, Wolfowicz I, Bechtoldt N, Guse A (2015) Induction
629 of Gametogenesis in the Cnidarian Endosymbiosis Model *Aiptasia* sp Sci Rep
630 5:15677 doi:10.1038/srep15677
- 631 Gruber B, Georges A, Berry O, Unmack P (2017) dartR: Importing and Analysing Snp and
632 Silicodart Data Generated by Genome-Wide Restriction Fragment Analysis. CRAN,
- 633 Hawkins TD, Hagemeyer JC, Warner ME (2016a) Temperature moderates the
634 infectiousness of two conspecific *Symbiodinium* strains isolated from the same host
635 population Environmental microbiology 18:5204-5217
- 636 Hawkins TD, Hagemeyer JCG, Hoadley KD, Marsh AG, Warner ME (2016b) Partitioning of
637 Respiration in an Animal-Algal Symbiosis: Implications for Different Aerobic Capacity
638 between *Symbiodinium* spp Frontiers in Physiology 7:128
639 doi:10.3389/fphys.2016.00128
- 640 Hillyer KE, Dias DA, Lutz A, Roessner U, Davy SK (2017) Mapping carbon fate during
641 bleaching in a model cnidarian symbiosis: the application of 13 C metabolomics New
642 Phytol 214:1551-1562 doi:10.1111/nph.14515
- 643 Hoadley KD, Rollison D, Pettay DT, Warner ME (2015) Differential carbon utilization and
644 asexual reproduction under elevated CO₂ conditions in the model

- 645 anemone, *Exaiptasia pallida*, hosting different symbionts *Limnology and*
646 *Oceanography* 60:2108-2120 doi:10.1002/lno.10160
- 647 Hoadley KD, Warner ME (2017) Use of Open Source Hardware and Software Platforms to
648 Quantify Spectrally Dependent Differences in Photochemical Efficiency and
649 Functional Absorption Cross Section within the Dinoflagellate *Symbiodinium* spp
650 *Frontiers in Marine Science* 4 doi:10.3389/fmars.2017.00365
- 651 Hothorn T, Bretz F, Westfall P, Heiberger RM, Schuetzenmeister A, Scheibe S, Hothorn MT
652 (2016) Package 'multcomp' Simultaneous inference in general parametric models
653 Project for Statistical Computing, Vienna, Austria
- 654 Howe PL, Reichelt-Brushett AJ, Clark MW, Seery CR (2017) Toxicity estimates for diuron
655 and atrazine for the tropical marine cnidarian *Exaiptasia pallida* and in-hospite
656 *Symbiodinium* spp. using PAM chlorophyll-a fluorometry *J Photochem Photobiol B*
657 171:125-132 doi:10.1016/j.jphotobiol.2017.05.006
- 658 Howells E, Beltran V, Larsen N, Bay L, Willis B, Van Oppen M (2012) Coral thermal
659 tolerance shaped by local adaptation of photosymbionts *Nature Climate Change*
660 2:116
- 661 Hughes TP et al. (2017) Global warming and recurrent mass bleaching of corals *Nature*
662 543:373-377 doi:10.1038/nature21707
- 663 Hughes TP et al. (2018) Global warming transforms coral reef assemblages *Nature* 556:492-
664 496 doi:10.1038/s41586-018-0041-2
- 665 ICZN (2017) Opinion 2404 (Case 3633) —*Dysactis pallida* Agassiz in Verrill, 1864 (currently
666 *Aiptasia pallida*; Cnidaria, Anthozoa, Hexacorallia, Actiniaria): precedence over
667 *Aiptasia diaphana* (Rapp, 1829), *Aiptasia tagetes* (Duchassaing de Fombressin &
668 Michelotti, 1864), *Aiptasia mimosa* (Duchassaing de Fombressin & Michelotti, 1864)
669 and *Aiptasia inula* (Duchassaing de Fombressin & Michelotti, 1864) not approved
670 *The Bulletin of Zoological Nomenclature* 74:130-132, 133
- 671 Kearse M et al. (2012) Geneious Basic: an integrated and extendable desktop software
672 platform for the organization and analysis of sequence data *Bioinformatics* (Oxford,
673 England) 28:1647-1649 doi:10.1093/bioinformatics/bts199
- 674 Kenkel CD, Bay LK (2018) Exploring mechanisms that affect coral cooperation: symbiont
675 transmission mode, cell density and community composition bioRxiv:067322
676 doi:10.1101/067322
- 677 Kumar S, Stecher G, Li M, Knyaz C, Tamura K (2018) MEGA X: molecular evolutionary
678 genetics analysis across computing platforms *Molecular biology and evolution*
679 35:1547-1549
- 680 LaJeunesse TC, Parkinson JE, Gabrielson PW, Jeong HJ, Reimer JD, Voolstra CR, Santos
681 SR (2018) Systematic Revision of Symbiodiniaceae Highlights the Antiquity and
682 Diversity of Coral Endosymbionts *Curr Biol* 28:2570-2580 e2576
683 doi:10.1016/j.cub.2018.07.008
- 684 Lehnert EM, Burriesci MS, Pringle JR (2012) Developing the anemone *Aiptasia* as a
685 tractable model for cnidarian-dinoflagellate symbiosis: the transcriptome of
686 aposymbiotic *A. pallida* *BMC Genomics* 13:271 doi:10.1186/1471-2164-13-271
- 687 Lehnert EM, Mouchka ME, Burriesci MS, Gallo ND, Schwarz JA, Pringle JR (2014)
688 Extensive differences in gene expression between symbiotic and aposymbiotic
689 cnidarians *G3 (Bethesda)* 4:277-295 doi:10.1534/g3.113.009084
- 690 Melville J et al. (2017) Identifying hybridization and admixture using SNPs: application of the
691 DArTseq platform in phylogeographic research on vertebrates *Royal Society open*
692 *science* 4:161061
- 693 Muller-Parker G, Cook CB, D'Elia CF (1990) Feeding affects phosphate fluxes in the
694 symbiotic sea anemone *Aiptasia pallida* *Marine Ecology Progress Series* 60:283-290
- 695 Muscatine L, Porter JW (1977) Reef corals: mutualistic symbioses adapted to nutrient-poor
696 environments *Bioscience* 27:454-460
- 697 Nei M, Kumar S (2000) *Molecular evolution and phylogenetics*. Oxford university press,

- 698 O'Mahony J, Simes R, Redhill D, Heaton K, Atkinson C, Hayward E, Nguyen M (2017) At
699 what price? The economic, social and icon value of the Great Barrier Reef. Deloitte
700 Access Economics, Brisbane, QLD, Australia
- 701 Perez SF, Cook CB, Brooks WR (2001) The role of symbiotic dinoflagellates in the
702 temperature-induced bleaching response of the subtropical sea anemone *Aiptasia*
703 *pallida* *Journal of Experimental Marine Biology and Ecology* 256:1-14
- 704 Pinheiro J, Bates D, DebRoy S, Sarkar D, Heisterkamp S, Van Willigen B, Maintainer R
705 (2017) Package 'nlme' Linear and Nonlinear Mixed Effects Models, version:3-1
- 706 Pochon X, Pawlowski J, Zaninetti L, Rowan R (2001) High genetic diversity and relative
707 specificity among Symbiodinium-like endosymbiotic dinoflagellates in soritid
708 foraminiferans *Marine Biology* 139:1069-1078 doi:10.1007/s002270100674
- 709 Rådecker N et al. (2018) Using *Aiptasia* as a Model to Study Metabolic Interactions in
710 Cnidarian-Symbiodinium Symbioses *Frontiers in physiology* 9:214-214
711 doi:10.3389/fphys.2018.00214
- 712 Ragni M, Airs RL, Hennige SJ, Suggett DJ, Warner ME, Geider RJ (2010) PSII
713 photoinhibition and photorepair in Symbiodinium (Pyrrhophyta) differs between
714 thermally tolerant and sensitive phylotypes *Marine Ecology Progress Series* 406:57-
715 70
- 716 Rapp W (1829) *Über die Polypen im Allgemeinen und die Actinien* Verlag des
717 Großherzoglich Sächsischen privileg Landes-Industrie-Comptoirs, Weimar
- 718 Rognes T, Flouri T, Nichols B, Quince C, Mahé F (2016) VSEARCH: a versatile open source
719 tool for metagenomics *PeerJ* 4:e2584
- 720 Rohwer F, Seguritan V, Azam F, Knowlton N (2002) Diversity and distribution of coral-
721 associated bacteria *Mar Ecol Prog Ser* 243:10
- 722 Rosado PM et al. (2018) Marine probiotics: increasing coral resistance to bleaching through
723 microbiome manipulation *The ISME Journal* doi:10.1038/s41396-018-0323-6
- 724 Schlesinger A, Kramarsky-Winter E, Rosenfeld H, Armoza-Zvoloni R, Loya Y (2010) Sexual
725 plasticity and self-fertilization in the sea anemone *Aiptasia diaphana* *PLoS One*
726 5:e11874 doi:10.1371/journal.pone.0011874
- 727 Stat M, Pochon X, Cowie RO, Gates RD (2009) Specificity in communities of Symbiodinium
728 in corals from Johnston Atoll *Marine Ecology Progress Series* 386:83-96
- 729 Steele RD (1976) Light intensity as a factor in the regulation of the density of symbiotic
730 zooxanthellae in *Aiptasia tagetes* (Coelenterata, Anthozoa) *Journal of Zoology*
731 179:387-405 doi:doi:10.1111/j.1469-7998.1976.tb02302.x
- 732 Suggett DJ, Warner ME, Smith DJ, Davey P, Hennige S, Baker NR (2008) Photosynthesis
733 and production of hydrogen peroxide by Symbiodinium (pyrrhophyta) phylotypes with
734 different thermal tolerances 1 *Journal of Phycology* 44:948-956
- 735 Sunagawa S et al. (2009) Generation and analysis of transcriptomic resources for a model
736 system on the rise: the sea anemone *Aiptasia pallida* and its dinoflagellate
737 endosymbiont *BMC Genomics* 10:258 doi:10.1186/1471-2164-10-258
- 738 Team RC (2013) R: A language and environment for statistical computing
- 739 Thornhill DJ, Xiang Y, Pettay DT, Zhong M, Santos SR (2013) Population genetic data of a
740 model symbiotic cnidarian system reveal remarkable symbiotic specificity and
741 vectored introductions across ocean basins *Mol Ecol* 22:4499-4515
742 doi:10.1111/mec.12416
- 743 Verrill AE Revision of the polypi of the eastern coast of the United States. In, 1864. Boston
744 Society of Natural History,
- 745 Wangpraseurt D, Larkum AW, Franklin J, Szabo M, Ralph PJ, Kuhl M (2014) Lateral light
746 transfer ensures efficient resource distribution in symbiont-bearing corals *J Exp Biol*
747 217:489-498 doi:10.1242/jeb.091116
- 748 Weis VM, Davy SK, Hoegh-Guldberg O, Rodriguez-Lanetty M, Pringle JR (2008) Cell
749 biology in model systems as the key to understanding corals *Trends Ecol Evol*
750 23:369-376 doi:10.1016/j.tree.2008.03.004

- 751 Wilson K et al. (2002) Genetic mapping of the black tiger shrimp *Penaeus monodon* with
752 amplified fragment length polymorphism *Aquaculture* 204:297-309
753 doi:[https://doi.org/10.1016/S0044-8486\(01\)00842-0](https://doi.org/10.1016/S0044-8486(01)00842-0)
754 Xiang T, Hambleton EA, DeNofrio JC, Pringle JR, Grossman AR (2013) Isolation of clonal
755 axenic strains of the symbiotic dinoflagellate *Symbiodinium* and their growth and host
756 specificity(1) *J Phycol* 49:447-458 doi:10.1111/jpy.12055
757 Ziegler M, Roder CM, Büchel C, Voolstra CR (2015) Mesophotic coral depth acclimatization
758 is a function of host-specific symbiont physiology *Frontiers in Marine Science* 2:4
759